The Mechanism of Lithium Zincate-Mediated I/Zn Exchange Revisited: A Computational Microsolvation Approach in THF**

Alexandre Pierret, Corentin Lefebvre, Philippe C Gros, Clément Denhez, Alexandre Vasseur

The Mechanism of Lithium Zincate-Mediated I/Zn Exchange Revisited: A Computational Microsolvation Approach in THF

Alexandre Pierret,[a] Corentin Lefebvre,[a] Philippe C. Gros,[a] Clément Denhez,*[b] and Alexandre Vasseur*[a]

Lithium trialkylzincate-mediated I/Zn exchange reaction has been revisited computationally through a microsolvation approach. A never yet investigated iodoaryl derivative bearing a potential bulky *para*-directing group, namely 4-iodobenzyl mesylate, was considered as a substrate. THF as typical solvent and Et_3ZnLi have also been considered for the first time in such a reaction. Three mechanistic pathways have been calculated, including (1) a literature-inspired pathway with full preservation of the synergic character of the reagent as well as a complementary mesylate group-directed pathway, (2) a THF-solvated open complex-promoted pathway and (3) an anionic pathway. While the anionic pathway appeared to be unlikely, pathway involving a THF-solvated open zincate complex turned out to be the most energetically favored. Equivalent thermodynamic profiles were found for both complementary pathways with preservation of the synergic character of the reagent, albeit a slight preference could be attributed to that occurring with initial chelation of Li to the mesylate group (OMs) through microsolvation approach. The I/Zn exchange was shown to proceed through a lithium-assisted aryl shuttle-like process. The iodoaryl substrate is first converted into ArLi intermediate which in turns reacts with the remaining diorganozinc reagent.

Introduction

The mechanism of the halogen/metal exchange reaction[1] has been debated intensively since the pioneering work of Gilman in this regard.[2] From that time onwards, no fewer than four proposals have been put forward and argued,[3] namely (1) a concerted four-centre transition state-based mechanism,[4] (2) a single electron transfer (S.E.T.) pathway,[5] (3) a so-called X-philic mechanism[6] involving a S_N2 reaction-like concerted transition state[7] and (4) an X-philic-like pathway with involvement of an ate complex as intermediate.[8] Nowadays, the debate is settled, at least for I/Li exchange process bringing into play $(RLi)_n$ as a homopolymetallic reagent and ArI as a substrate.[9] It appears clear that such a reaction proceeds through the proposal (4) as evidenced by numerous spectroscopic studies in which the ate complex intermediate has been observed.[10] Moreover, a plethora of computational studies[11] and even a solid-state structure of the key intermediate obtained by X-ray crystallography[12] provide strong credibility to this mechanistic rationale. In contrast, mechanisms behind the I/metal exchange reaction promoted by heterobimetallic organoreagents $[R_nM^1]^-$-$[(M^2)_{n-2}]^+$ have been discussed with far less enthusiasm. This is probably due to a challenging understanding of such synergic reagents' behaviour in solution.[13] Indeed, current mechanistic data are often deduced from solid-state structural analysis of bimetallic intermediates individually characterised by X-ray diffraction. This approach can obviously be inspiring for setting up reliable and convincing mechanistic assumptions.[14] However, possible solvation state changes of the involved organometallic intermediates in solution as well as related variations of their aggregation state and geometry have to be carefully considered. As a matter of fact, the synergic character of heterobimetallic reagents may deeply be altered in solution as demonstrated by ^{1}H- and ^{13}C-NMR investigations of the deproto-metalation of *N*-Phenylpyrrole by the putative $LiZn(TMP)_3$ reagent followed by iodolysis[15] and by DOSY analysis in other similar transformations.[16] Since the results strongly depend on reaction conditions, namely both the used solvent and substrate, kinetic studies may deliver contradictory outcomes.[17] On another side, quantum chemistry calculations using Density Functional Theory (DFT) may be a powerful mechanistic investigation tool providing that influences of key parameters (*e.g.* solvent, substituents and functional groups within the substrate and/or the reagent, salts) on the structure-reactivity relationship of the heterobimetallic reagent are thoroughly examined.[18] Nevertheless, computational studies on halogen/metal exchange promoted by such a reagent-type[19] are available and have been carried out (1) in the absence of functional group on the substrate (2) in unusual solvent (Me_2O instead of the most commonly used THF) and (3)

[a] *Dr. A. Pierret, Dr. C. Lefebvre, Dr. P. C. Gros, Dr. A. Vasseur*
Université de Lorraine
CNRS, L2CM,
F-54000 Nancy -France-
E-mail: alexandre.vasseur@univ-lorraine.fr

[b] *Dr. C. Denhez*
Université de Reims Champagne Ardenne
CNRS, ICMR UMR 7312,
51097 Reims, France
E-mail: clement.denhez@univ-reims.fr

without relying on the microsolvation approach, likely because the determination of the suitable number of solvent molecules coordinated to intermediates and transition states represents a tedious work.[18]

In this paper, we have computationally reinvestigated the mechanism of the I/Zn exchange reaction of 4-iodobenzyl mesylate (**1 a**) with Et_3ZnLi in THF at 188.15 K (Scheme 1) and by considering the microsolvation approach. **1 a** has been selected as a model substrate owing to its synthetic potential highlighted in previously reported transformations based on a remote functionalisation tactic.[20] In addition, the bulky mesylate group (OMs) may play the role of *para* directing group and therefore influence the mechanism. Simply put, our microsolvation approach allowed stating that Et_3ZnLi with two THF molecules coordinated to Li is the most likely structure when such a reagent is placed in a THF solution. $Et_3ZnLi\cdot 2THF$ was identified as a versatile species. This versality was illustrated by several computationally characterised limit forms. The first one, with the highest statistical weight, corresponded to a $Et_3ZnLi\cdot 2THF$ structure in which Li.2THF was positioned equidistantly between its two L-type C_{Et} ligands. The second one had a structure in which Li was moving between its two L-type C_{Et} ligands. The third one, with the lowest statistical weight, was an original THF-solvated open zincate complex consisting of two distinct complexes, Et_2Zn and EtLi, and two THF molecules, each of them coordinating both metal centres. Several interconnected dynamic equilibria between variously THF solvated Et_3ZnLi were found and then considered to investigate three reactional pathways. Our conclusion was that the pathway promoted by a transiently formed THF-solvated open zincate complex (pathway 2a–b) was thermodynamically more favourable than the literature-inspired pathway with full preservation of the synergic character of the reagent (pathway 1a–c). The OMs group did not seem to play a significant role in the mechanism (pathway 1d–f, complementary to pathway 1a–c). Either way, we demonstrated that the I/Zn exchange occurred through a two-step process. Firstly, the iodoaryl substrate was converted into ArLi intermediate. Then, ArLi reacted with the remaining diorganozinc species so as to form the expected I/Zn exchange product. An anionic pathway (pathway 3a-b), requiring a preliminary dissociation of $Et_3ZnLi\cdot 2THF$ into $[Et_3Zn]^-$ and $[Li(THF)_2]^+$, was also calculated and proved to be the least energetically favourable among all the considered options.

Results and Discussion

Structure of Et_3ZnLi in THF

All structures were fully optimised with the M06-2X DFT functional[21] with aug-cc-pVDZ basis set[22] for all atoms except I where ECP card was used with the SDD basis set. The D3 version of Grimme's dispersion correction with the original D3 damping function was added for all calculations.[23] In addition to the THF solvent molecules bound to the metals, implicit solvation in THF was used using the Integral Equations Formalism version of the Polarisable Continuum Model (IEFPCM),[24] (See SI). The anionic zinc moiety adopts a common trigonal planar geometry, the sum of the Et-Zn-Et angles being 360 ± 0.8° (Scheme 2 and Figure SI.3.). Two of the three Et groups bridge to Li cation through their Cα atoms and the average of calculated Zn–Cα bond lengths is 2.12 Å. On the whole, all calculated geometrical parameters of **A** are in line with solid-state structural data reported for its analog *t*-$Bu_3ZnLi(hpp)_6$[25] and other alkali metal trialkylzincates.[26] Previously disclosed ^{1}H NMR analysis of **A** prepared in benzene solution by reacting EtLi and Et_2Zn revealed that such a complex featured the formula $Et_3ZnLi\cdot 2THF$ when more than 2 equivalents of THF were added.[27] This study as well as the ESI(-)-MS analysis of a THF solution of Bu_3ZnLi[28] also suggest that **A** exists in monomeric form in this solvent. Lastly, crystallographic data for triorganozincate complexes disclosed that THF can coordinate either the metal cation[29] or the Zn centre,[30] hence the importance of calculating all possible combinations so as to determine the most stable solvated structure for **A**. Coordination of one or two molecules of THF to the Li atom of **A** leads to **B** or **C** with a large energy gain (**B**, 8.1 kcal/mol and **C**, 15.8 kcal/mol). **C** is more stable than **D** featuring only one molecule of THF coordinated to the Zn centre and **E** possessing two molecules of THF at both the Zn centre and the alkali metal by 13.8 kcal/mol and 4.3 kcal/mol respectively. Those results are in good agreement with the experimental observation that **A** adopts a $Et_3ZnLi\cdot 2THF$ composition when placed in a THF solution. This composition therefore refers to **C** rather than **E**, albeit the difference in energy remains reasonably low. We also modelled some unusual species that are not reported in the solid-state structural database but sometimes suggested in some computational mechanistic studies. For instance, **F** with only one Et group bridging Li cation through its Cα atom, is disfavoured by only 5.9 kcal/mol with respect to **C**. In this structure, the Li cation is in almost perfect alignment with one of the three Cα and the Zn centre (angle value of 166.1°, Figure SI.3.). It should be stressed that this open-form zincate was already supposed to be involved in the conjugate addition reaction of lithium

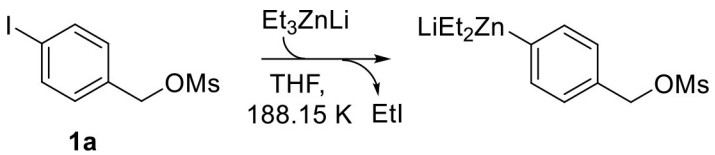

1a

Scheme 1. Computationally studied I/Zn exchange reaction.

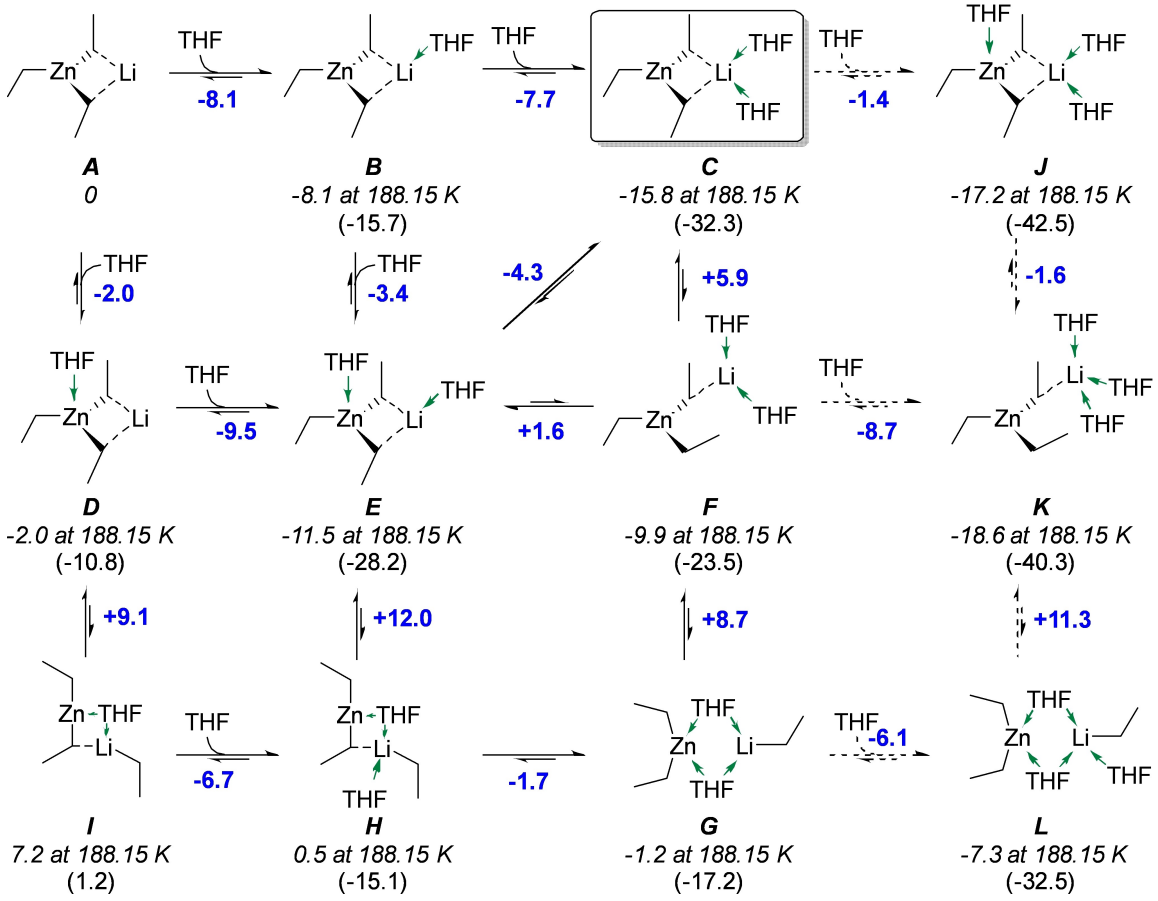

Scheme 2. Structural determination of $Et_3ZnLi{\cdot}nTHF$ formula through microsolvation approach at the IEFPCM/M06-2X-D3/cc-pVDZ level of theory (Gibbs free energies at 188.15 K and enthalpies in parentheses are specified in kcal/mol. ΔG° are accessible in the SI).

organozincates to *s-trans*-enones.[31] **F** may evolve towards the doubly THF-solvated open complex **G** resulting from the dissociation of Et_3ZnLi into Et_2Zn and EtLi. If so, such a dissociation process would occur with 8.7 and 14.6 kcal/mol endergonicity *vis-à-vis* **F** and **C** respectively. This kind of species was regarded in the computed reaction pathway of 1,2-addition of Me_3ZnLi reagent to formaldehyde but was deemed unlikely since this chemical event was associated with the 24.2 kcal/mol loss of electronic energy in Me_2O as solvent.[32] Comparatively in THF as solvent, similar dissociation is about 10 kcal/mol lower in electronic energy (see tables in SI) and cannot therefore be precluded as easily. The reorganisation of **G** into **H** should proceed smoothly since it is almost barrierless (only 1.7 kcal/mol) whereas the formation of **I** resulting from the decoordination of one solvent molecule from Li is more energy demanding. Although not suspected by NMR analysis in THF, calculation results related to complexes with statured coordination sphere at both metal centres are given for information only (**J**–**L**). Broadly speaking, coordination of a third molecule of THF either to the Zn centre of **C** or to the Li cation of **F** affords **J** or **K** respectively with a modest (1.4 kcal/mol for **J**) to important (8.7 kcal/mol for **K**) gain in energy. In contrast, coordination of an additional THF to Li in **G** results in a notable Gibbs free energy gain (6.1 kcal/mol, see **L**) which would provide credit to the existence of such a species in solution by helping to shift the equilibrium from **C** towards **G**. As the equilibrium **C**⇌**F**⇌**G** proposed in Scheme 2 suggests that alkali metal of the versatile species **C** is moving between its two L-type C_{Et} ligand, we took a close look at the involved intrinsic bond strengths by using the recent independent gradient model (IGM) and its δg descriptor-based Intrinsic Bond Strength Index (IBSI)[33] (Scheme 3). This recently developed methodology allows a quick quantification and qualification of bonds in molecules and is a new remarkable tool for the description of transition states. The average of calculated IBSI values for the two C_α–Zn bonds adjacent to the Li cation (0.203) indicates a covalent character which is 33% lower than for the C_α-bond opposite the Li atom. Two other bond strengths could be estimated with the IBSI, namely the C_α-Li and the heterobimetallic Zn–Li bonds. Both are notable for a low IBSI value (0.063 on average and 0.066 respectively). The charge transfer interaction from CH_2 attached to Zn ($C_\alpha H_\alpha$) and the neighbouring Li was estimated to be around 5 kcal/mol by $E^{(2)}$ (second order perturbation energy) energy Natural Bond Orbital (NBO) calculation. Given these low IBSI values, the low endergonicity relating to the formation of **F** from **C** (5.9 kcal/mol) is not surprising. Moreover, a stability gain is brought by additional $C_\beta H_\beta$ agostic interactions, hence the $E^{(2)}$ energy NBO value (8.3 kcal/mol) greater than that found in **C**

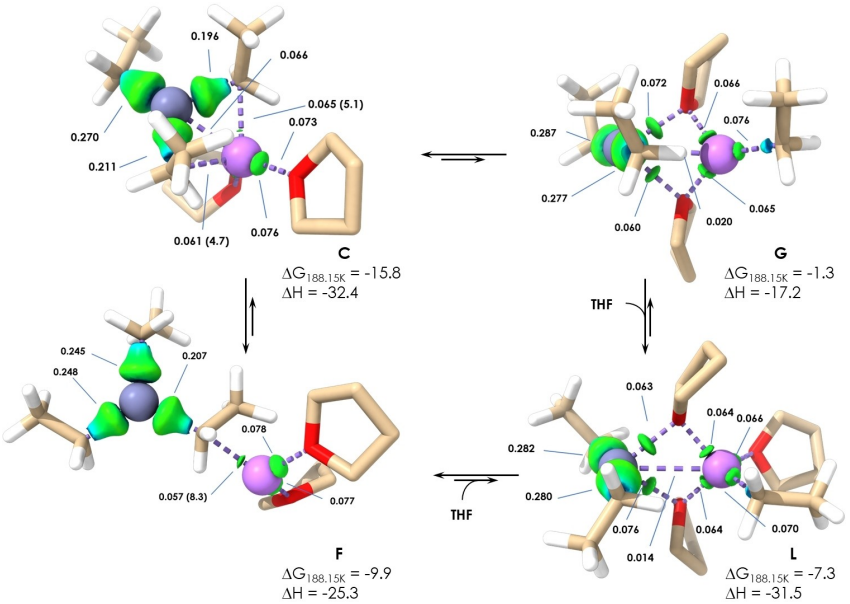

Scheme 3. 3D representation of the equilibrium between $Et_3ZnLi{\cdot}nTHF$ species with IBSI values. (Energies values in kcal/mol, $E^{(2)}$ energies in parentheses. Zn atom is represented as a blue sphere and Li atom as a purple sphere, H atoms of THF molecules are omitted for better clarity. ΔG° are accessible in the SI).

(5 kcal/mol). The IBSI value of the C_α–Li bond in **F** is of the same order as that in **C**. Consequently, the alkali metal should easily move from its central position to one or the other close α-carbon atom and then return to its earlier position as depicted in Figure 1. Also, the covalent nature of the C_α–Zn bond in the vicinity of Li noticed in **C** is maintained in **F** (IBSI value of the same order: 0.207 in **F** versus an average of 0.204 in **C**). Therefore, only 8.7 kcal/mol is required for the transfer of the ethyl ligand from Zn to Li furnishing **G**. This endergonicity is even reverted to 2.6 kcal/mol if the triply THF solvated complex **L** is considered. **G** could actually be seen as a diethylzinc complex associated with a monomeric EtLi complex by two THF solvent molecules since the covalent character of the C_α–Zn bond (IBSI = 0.280) significantly increases with respect to that observed in similar bonds of the purely ate complex **C** (IBSI = 0.225 on average). Nevertheless, it could also be viewed as a THF-solvated open zincate complex on account of the preservation of an interaction between both metals (IBSI = 0.020), though significantly weaker than that observed in **C**. The endergonicity of the formation process of **G** can be mainly explained by the loss of agostic C_αH Interactions which is not compensated by the formation of new coordination bonds. In contrast, the coordination of an additional THF to Li as in **L** enables a compensation. Once again, the versatility of $Et_3ZnLi \cdot 2THF$ is illustrated by this another limit form **G** where an ethyl ligand could be dynamically exchanged from Zn to Li atoms (Figure 1). Based on IBSI analysis of **C** and reported data deduced from solid-state structural analysis of lithium trialkylzincates suggesting that alkyl ligands are covalently bonded to Zn centre,[34] **G** should unquestionably be the limit form with the lowest statistical weight compared to that of **C** or **F**. Thus, **G** should be seen only as a transient species.

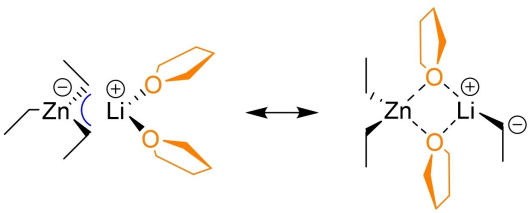

Figure 1. Calculated limit forms of $Et_3ZnLi \cdot 2THF$.

In the light of these calculations, **C** was selected as the model zincate species for the next phase of the study. Three reaction pathways were investigated through microsolvation approach (Scheme 4). The first studied route involves both equilibria **C**⇌**B** and **C**⇌**E** without (pathway 1a–c, Scheme 4) or with consideration of the influence of mesylate group as a potential directing group (pathway 1d-e, Scheme 7). The second calculated route draws on the equilibrium **C**⇌**G**⇌**I** (pathway 2a–b, Scheme 8) whereas the last one corresponds to an anionic pathway (pathway 3a–b, Scheme 10) initiated by dissociation of **C** into isolated zincate $[Et_3Zn]^-$ and lithium solvated cation $[Li(THF)_2]^+$.

I/Zn exchange reaction pathway with preserved synergic character of $Et_3ZnLi \cdot 2THF$

Efforts for contacting the reactants **C** and **1a** *via* Li–I interaction led to the formation of the association complex $\mathbf{CP_{1a}}$ (Scheme 4) with a small Gibbs free energy gain (2.8 kcal/mol, pathway 1a). In contrast with a previous computational report on the I/Zn exchange reaction between EtI and Me_3ZnLi in Me_2O,[19a] the iodine cannot be coordinated to the Li centre due to a longer distance (3.93 Å versus 3.12 Å, Figure SI.4.). Independent

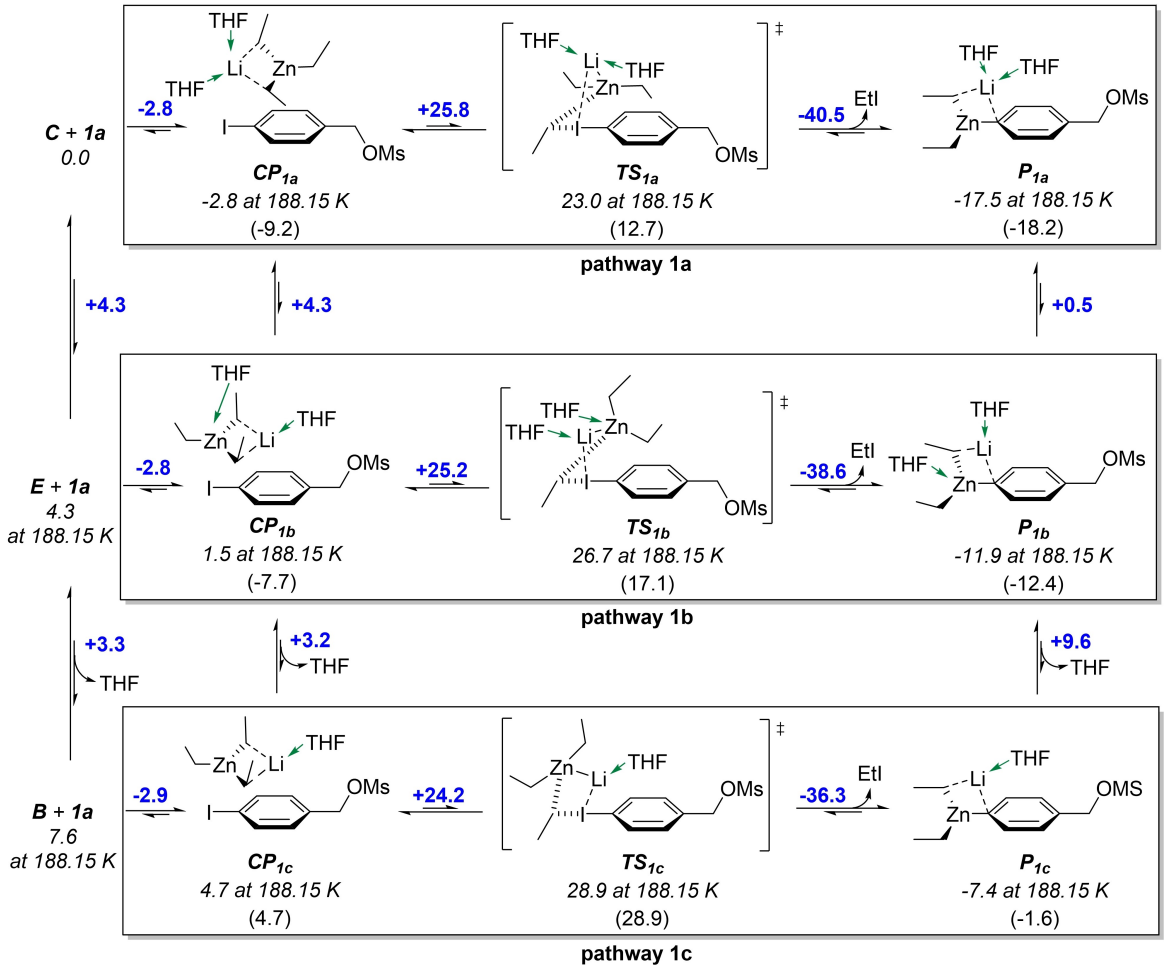

Scheme 4. I/Zn exchange reaction pathway with preserved synergic character of $Et_3ZnLi \cdot 2THF$ calculated at the IEFPCM/M06-2X-D3/cc-pVDZ (SDD for I) level of theory (Gibbs free energies at 188.15 K and enthalpies in parentheses are specified in kcal/mol. ΔG° are accessible in the SI.

gradient model (IGM) analysis of non-covalent intermolecular interactions[35] only revealed dispersion interactions between the C–H moiety of a THF molecule and the iodine atom on one hand and between alkyl ligands and the π-system of the aromatic cycle on the other hand (See Figure SI.8.). However, computed NBO analysis indicated a 5 kcal/mol $E^{(2)}$ energy stabilisation between the lone pair of I and the lone vacant orbital of Li. Changes in the solvation degree of Li and Zn centres by external THF molecules led to $\mathbf{CP_{1b}}$ (with one solvent molecule coordinated to Zn metal while another one remains coordinated to Li) and $\mathbf{CP_{1c}}$ (with only one THF bound to Li) energetically destabilised by 4.3 and 7.5 kcal/mol respectively with respect to $\mathbf{CP_{1a}}$. It should be stressed that the solvation state of $\mathbf{CP_{1b}}$ induces a 180° reversal of the aromatic ring moiety when compared with $\mathbf{CP_{1a}}$. In spite of a now permitted interaction between the lone pair of the iodine atom and the lone vacant orbital of the Zn metal centre ($E^{(2)}$ computed energy NBO of 7.8 kcal/mol), this event is not sufficient to favour $\mathbf{CP_{1b}}$ vis-à-vis $\mathbf{CP_{1a}}$. The geometrical parameters of **C** are essentially retained in the heterobimetallic reagent interacting with **1a** (See Figure SI.4.). Among the three ethyl ligands, those bridging the Li cation are equivalent. Migration of one of them proceeds smoothly along the intrinsic reaction coordinate to the iodine atom with an activation Gibbs free energy of 25.8 kcal/mol from $\mathbf{CP_{1a}}$ so as to afford $\mathbf{TS_{1a}}$. Although the Zn-C_{Et} bond cleavage is not partially compensated by the formation of a Zn–I bond like in the calculated TS for the I/Zn exchange reaction between Me_3ZnLi and EtI in Me_2O,[19a] this value is about 7 kcal/mol lower in energy (25.8 vs 34.1 kcal/mol). This difference in energy could be expected since R_3ZnLi preferentially reacts with primary alkyl iodides through nucleophilic substitution rather than I/Zn exchange reaction. $\mathbf{TS_{1a}}$ exhibits all characteristics of a hypervalent halogen-type structure, namely a C_{Et}–I–C_{Ar} angle approaching 180° hence C_{Et} directly positioned in front of the σ-hole of the iodine atom (See MEP analysis of **1a**, Figure SI.1.) and two covalent C_{Et}–I and C_{Ar}–I bonds. This electron-deficient region arises from the anisotropic electron density distribution of atoms of group 14–17 elements covalently bounded to electron withdrawing groups. The σ-hole has been intensely studied and was shown to govern the interactions and the reactivity of these bounded elements.[36] As previously mentioned, a weak interaction between Zn and Li could be detected by IBSI analysis in the structure of **C** (IBSI value = 0.066, Scheme 3). This heterobimetallic bond is maintained in $\mathbf{TS_{1a}}$,

although the calculated IBSI value is lower (IBSI value = 0.026), showing that both metals participate in the transition state. Accordingly, this I/Zn exchange reaction pathway appears as a lithium-zinc-mediated transformation in which Li and Zn act synergistically as if they formed a unique "Lithium zincate" element, in accordance with the "pairiodic" table of the elements proposed by Mulvey et al.[13a] The drastic changes in IBSI values of the reactive Cα-Zn bond from **CP$_{1a}$** (0.204) to **TS$_{1a}$** (0.081) are considered to demonstrate the ongoing cleavage of the C$_{Et}$–Zn bond in **TS$_{1a}$** so as to position the ethyl ligand in front of the σ-hole of the iodine atom (Schemes SI.1. and SI.2.). The IBSI values relating to the C$_{Ar}$–I (0.335 in **CP$_{1a}$** and 0.184 in **TS$_{1a}$**) and C$_{Et}$–I (0.005 in **CP$_{1a}$** and 0.195 in **TS$_{1a}$**) simultaneously decreases and increases respectively suggesting a C$_{Ar}$–I bonding character loss concomitantly to the formation of a new C$_{Et}$–I bond. Similar conclusions were reached for pathway 1b, except this time round the ethyl transfer process is more advanced in **TS$_{1b}$** (IBSI values are 0.005 for the Cα–Zn bond and 0.230 for the C$_{Et}$–I bond) than in **TS$_{1a}$** (Scheme SI.2.). Lastly, atomic orbitals of C$_{Et}$, C$_{Ar}$ and I form three molecular orbitals (See Figure SI.9.): a bonding orbital (*e.g.* HOMO-9), an anti-bonding orbital (*e.g.* LUMO + 8), and an unoccupied non-bonding orbital HOMO (interaction between 2p$_z$ orbitals of C$_{Ar}$ and ethyl groups), which is typical of a three-centre four-electron bond encountered in hypervalent iodine-type structures.[37] Gibbs free energies of activation corresponding to the three differently solvated **TS$_{1a-c}$** are similar but **TS$_{1a}$** has the lowest potential Gibbs free energy (23.0 vs 26.7 for **TS$_{1b}$** and 28.9 kcal/mol for **TS$_{1c}$**). Natural population charge changes in pathway 1a show that the negative charge of C$_{Ar}$ increases in **TS$_{1a}$** with respect to **CP$_{1a}$**, the positive charge of Zn and Li being unchanged (see Figure SI.10.). Consequently, a transfer of the aryl moiety to the Zn centre can produce the final I/Zn exchange adduct **P$_{1a}$** with a stabilisation energy of 40.5 kcal/mol. The formed lithium dialkylarylzincate **P$_{1a}$** is only slightly more stable than its analogue **P$_{1b}$**, with one molecule of THF coordinated to Li and another coordinated to Zn, but it is much more stable than **P$_{1c}$** possessing only one single solvent molecule coordinated to Li. Since the C$_{Ar}$–Li distance (4.34 Å) is 11% shorter than the distance between C$_{Ar}$ and Zn (4.87 Å) in **TS$_{1a}$**, we reckoned that a transfer of the aryl moiety to Li was a rational prerequisite for the formation of **P$_{1a}$** (see geometrical parameters in Figure SI.5.). Gratifyingly, **INT$_{1a}$** corresponding to this transient transfer could be successfully localised as shown in Scheme 5. From **TS$_{1a}$**, the migration of the aryl moiety to the Li cation produces **INT$_{1a}$** with 25.2 kcal/mol stabilisation. A subsequent transfer of the aryl fragment to Zn finally produces **P$_{1a}$** with 15.3 kcal/mol stabilisation. To our knowledge, this likely crucial Li-assisted aryl shuttle-like process has not been reported yet.[38] It tends to demonstrate that the conversion of ArI into Ar(Et)$_2$ZnLi by the lithium triorganozincate starts with a iodine-lithium exchange of ArI into ArLi. Differently solvated **INT$_{1b}$** and **INT$_{1c}$** resulting from **TS$_{1b}$** and **TS$_{1c}$** respectively turned out to be energetically less favourable.

An alternative mechanistic route with preserved synergic character of the heterobimetallic reagent could also be the OMs-directed I/Zn exchange. If so, it could be similar to the

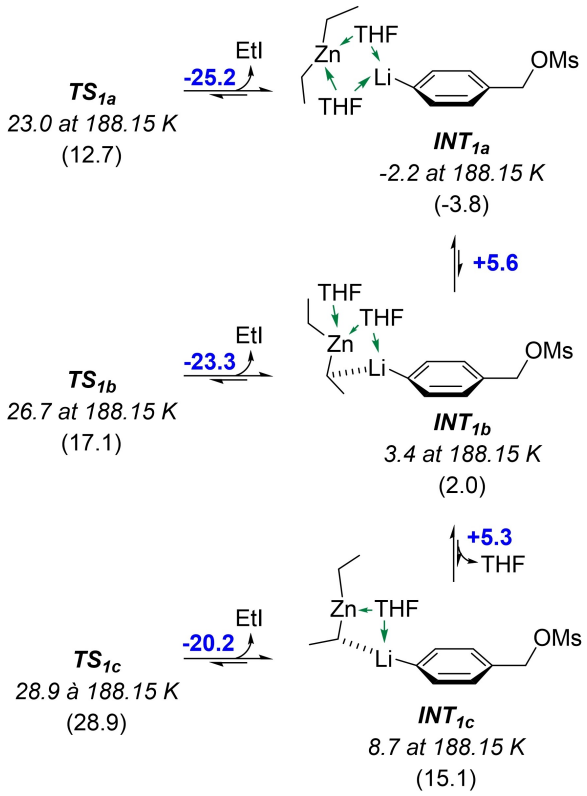

Scheme 5. Li-assisted aryl shuttle-like process calculated at the IEFPCM/M06-2X-D3/cc-pVDZ (SDD for I) level of theory (Gibbs free energies at 188.15 K and enthalpies in parentheses are specified in kcal/mol. ΔG° are accessible in the SI).

proposed keto-directed 1,4 or 1,2-addition of Me$_3$ZnLi to *s-trans*-enones involving an open form or closed form-like organozincate structure-based transition state.[31] Moreover, the presence of an oxygen atom on the aromatic ring was originally suspected to impact the Li/Br exchange mechanism owing to potential strong Li–O interactions weakening the strength of R–Li electrostatic bond.[6] The potential influence of the OMs group is experimentally difficult to assess. In particular, attempts to thoroughly monitor the kinetic of the conversion of the substrate **1a** (X = OMs) into Et$_2$(Ar)ZnLi by GC/MS or ^{1}H-NMR failed because unavoidable changes in the temperature systematically led to the formation of the corresponding homologated benzylic zinc intermediate.[20] Moreover, inconsistent outcomes were found for I/Zn exchange reactions performed with substrates bearing substituent other than OMs (Scheme 6). Whereas the treatment of **1a** (X = OMs) or **1b** (X =

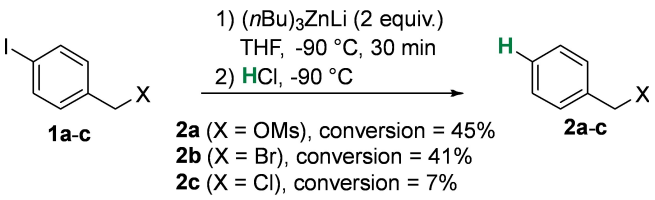

Scheme 6. I/Zn exchange reaction involving varied 4-iodobenzyl derivatives.

Br) with 2 equiv. of $(n\text{-Bu})_3ZnLi$ in THF at −90 °C during 30 min followed by addition of HCl led to the hydrolyzed I/Zn exchange product **2a** or **2b** with a similar GC/MS-calculated conversion (45 % or 41 % respectively), the reaction conducted with **1c** (X = Cl) as a substrate under identical conditions produced **2c** with **1c** being converted in 7 % only. Given this, only a computational approach appears reliable for examining a potential influence of the OMs group and complementary investigations were performed in this regard.

Coordination of one oxygen atom of the mesylate group to Li in $\mathbf{CP_{1a}}$ inevitably results in the loss of one solvent molecule to yield $\mathbf{CP_{1d}}$ with a very small ΔG gain (Scheme 7, 0.9 kcal/mol). No extra coordination of a THF molecule to alkali metal of $\mathbf{CP_{1d}}$ could be contemplated because of a high steric congestion. Besides, considering the OMs group as a O,O′ donor ligand of Li resulted in the decoordination of one of the two oxygen atoms after geometry optimisation. However, coordination of an additional THF molecule to the Zn centre of $\mathbf{CP_{1d}}$ allows the formation of the more stable complex $\mathbf{CP_{1e}}$ whereas total desolvation of the latter leads to a 14.4 kcal/mol loss of Gibbs free energy ($\mathbf{CP_{1f}}$). $\mathbf{CP_{1e}}$ displays a better stability than $\mathbf{CP_{1d}}$ owing to the strong electrostatic O–Li interaction that widely offsets the absence of the 2-electron interaction between I and Li. Furthermore, additional dispersion interactions between CH moieties of alkyl ligands of Zn and THF with oxygens of the OMs group and iodine may contribute to this small energy gain (see IGM analysis in Figure SI.8.). Overall, geometrical parameters of organometallic reagent **E** are maintained in $\mathbf{CP_{1e}}$ (identical C_{Et}–Zn–C_{Et} angles and C_{Et}–Zn bond lengths, See Figure SI.4.). One of the ethyl ligands is located at the vicinity of the iodine atom in this structure (4.0 Å distance). Thus, the direct ethyl transfer from the central Zn to the σ-hole of the iodine atom may take place through the transition state $\mathbf{TS_{1e}}$ so as to generate the I/Zn exchange complex $\mathbf{P_{1e'}}$ which is 35.1 kcal/mol lower in Gibbs free energy than $\mathbf{TS_{1e}}$. The required Gibbs free energy of activation is similar to that needed for the production of $\mathbf{P_{1d}}$ and $\mathbf{P_{1f}}$ (pathway 1e) through $\mathbf{TS_{1d}}$ and $\mathbf{TS_{1f}}$ respectively (pathway 1d and 1f), but $\mathbf{TS_{1e}}$ and the resulting $\mathbf{P_{1e}}$

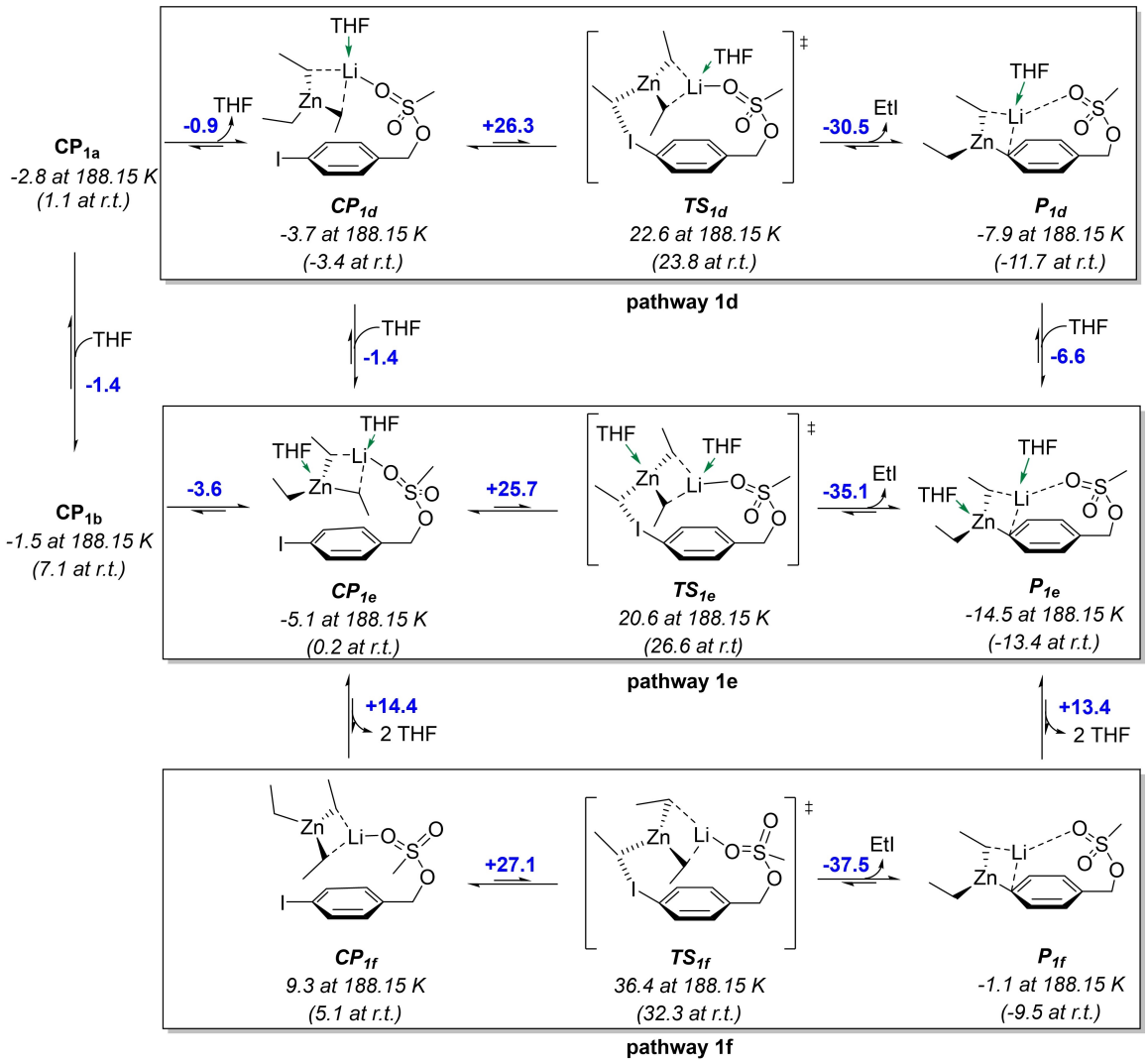

Scheme 7. OMs-directed I/Zn exchange reaction pathway calculated at the IEFPCM/M06-2X-D3/cc-pVDZ (SDD for I) level of theory (Gibbs free energies at 188.15 K and enthalpies in parentheses are specified in kcal/mol. ΔG° are accessible in the SI).

are localised at a lower potential Gibbs free energy. Therefore, pathway 1e represents the most favourable route when compared with the pathways 1d and 1f. Since the C_{Et}–I–C_{Ar} angle is around 170° and the selected suitable Kohn-Sham orbitals HOMO, HOMO-10 and LUMO+6 have the same features as HOMO, HOMO-9 and LUMO+8 described for **TS1$_{1a}$**, **TS$_{1e}$** has also a hypervalent iodine-type structure with a three-centre four-electron bond (see Figure SI.9.). As opposed to **TS$_{1a}$**, no interaction between the lone pair of I and the lone vacant orbital of Li could be made out via IGM analysis in **TS$_{1e}$**, but computed NBO analysis revealed a second order perturbation energy of stabilisation of 17.7 kcal/mol, which signals a 2-centre-2-electron stabilising interaction. The C_{Et}-I bond length (2.63 Å) is 20% greater than that of I–Ar (2.27 Å), which could mean that **TS$_{1e}$** is an early transition state (See Figure SI.5.). However, three common points between the pathway 1a and 1e can be identified. First, natural population charge changes in the reaction pathway 1e are quite similar as those computed in the reaction pathway 1a: the negative charge of C_{Ar} decreases whereas the positive charge of Li slightly increases during the changeover from **CP$_{1e}$** to **TS$_{1e}$**, hence a facilitated aryl moiety transfer to Li or Zn. Second, C_{Ar} is much closer to Li (2.82 Å) than to Zn (4.79 Å). Third, the changes in the IBSI values are similar to those noted in the pathway 1a (See Scheme SI.5). As a consequence, two conclusions can be drawn: (1) Li should act as a promotor of the generation of aryl anion, hence the release of ethyl iodide, (2) the Ar moiety should be first transferred to Li and after to Zn as explained in Scheme 5. With this in mind, calculated pathway 1e can be considered as complementary to pathway 1a since both are energetically equivalent with only a marginal preference for pathway 1e. Therefore, the OMs group does not play a significant role in the I/Zn exchange. A plausible explanation for the reactivity difference between **1a** and **1c** could be the formation of complex polynuclear zincate complexes promoted by the presence of the Cl atom[39] and that would be inactive for such reaction under our conditions. In any event, the most stable I/Zn exchange complex produced through this complementary OMs-directed pathway is **P$_{1e}$** solvated by two solvent molecules, namely one coordinated to Li while another is coordinated to the Zn centre.

THF-solvated open complexes-mediated pathway

With these results in hand, we then focussed on the possible involvement of solvated open complexes **G** and **I** (Scheme 2) previously defined as transient species where EtLi and Et_2Zn are respectively maintained in interaction thanks to THF molecules (Scheme 8). Indeed, the Gibbs free energy cost associated with the formation of **I** is similar to the Gibbs free energy of activation required for **TS$_{1a}$** and **TS$_{1e}$** while the energy cost related to **G** is 6.0 and 8.4 kcal lower respectively. If **G** and **I** exist in solution, they should not release free EtLi because the treatment of THF solution of **1a** and $ZnCl_2$ with 3 equivalents of EtLi experimentally led to a complex mixture. This experimental result was also confirmed when *n*-BuLi was used instead of EtLi. The reactants **1a** and **G** (or **I**) smoothly form an association complex **CP$_{2b}$** (or **CP$_{2a}$** if **I** is considered) without any gain or loss in energy. **CP$_{2b}$** clearly appears to be more thermodynamically stable than **CP$_{2a}$** produced from **I** and **1a**. Interestingly, the

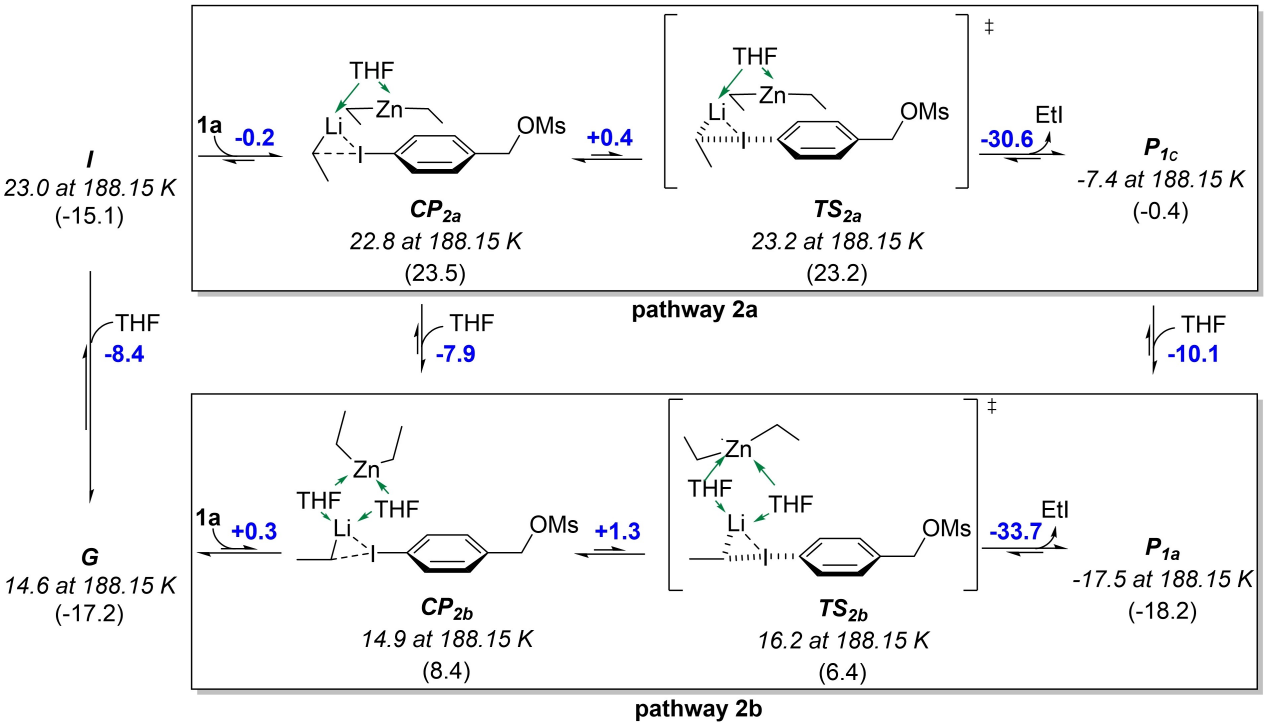

Scheme 8. THF-solvated open complex-mediated pathway calculated at the IEFPCM/M06-2X-D3/cc-pVDZ (SDD for I) level of theory (Gibbs free energies at 188.15 K and enthalpies in parentheses are specified in kcal/mol. ΔG° are accessible in the SI).

former exhibits the essential features of a hypervalent halogen-type structure and the Cα of the migratory ethyl ligand is already well positioned with regard to the σ-hole of the iodine atom. The IGM analysis disclosed that C_{Et} bonded to Li strongly interacted with iodine atom in an electrostatic manner (see Figure SI.8.) because of the short distance between both (2.95 Å, Figure SI.4.). Moreover, an interaction between I and Li could be viewed via this analysis method. In concrete terms, it refers to a second order perturbation energy of stabilisation of 31 kcal/mol between the lone pair of I and the lone vacant orbital of Li according to computed NBO analysis. Combining these observations with the C_{Et}–I–C_{Ar} angle close to 180°, **CP_{2b}** can be considered as a quasi-transition state. This is also confirmed by examination of the IBSI (Scheme 9) which shows (1) simultaneous interactions of the Cα of the migratory ethyl ligand with both Li (0.048) and iodine (0.063) atoms, (2) a significant reduction of the C_{Ar}–I bond strength (IBSI value = 0.051) with respect to that of the substrate **1a** (IBSI value = 0.302). Therefore, it is not surprising that only 1.3 kcal/mol are enough to reach **TS_{2b}** that is a three-centre four-electron bond of a hypervalent iodine-type structure as confirmed by selected suitable Kohn-Sham orbitals (see in Figure SI.9. the HOMO consisting mainly of the nonbonding interaction between $2p_z$ orbitals of the aryl and ethyl group, antibonding LUMO + 7 and bonding HOMO-8). In this TS structure, the C_{Ar}–I bond length is 8% longer than in **1a** foreshadowing a dissociation (IBSI value of 0.204). The distance between C_{Ar} and Li is considerably shorter than the C_{Ar}–Zn distance (2.76 Å versus 6.55 Å, Figure SI.5.). Consequently, the I/Zn exchange product **P_{1a}** stemming from the Ar–I bond cleavage should be formed after initial transfer of the Ar moiety to Li (Scheme 9), *i.e. via* **INT_{1a}** (Scheme 5) generated with a Gibbs free energy of stabilisation of 18.4 kcal/mol with respect to **TS_{2b}**. The slight decrease of the natural population charges of C_{Ar} in **TS_{2b}** with respect to that of C_{Ar} in **CP_{2b}** and the simultaneous opposite evolution of the natural population charge of Li may be the driving force for the formation of this key intermediate.

Calculated anionic pathway

Although already considered as very unlikely, we however investigated the anionic pathway involving the initial dissociation of **C** into $[Li(THF)_2]^+$ and isolated zincate **M** (pathway 3, Scheme 10). Only 17.6 kcal/mol free Gibbs energy is needed for this preliminary step, thus in sharp contrast with previously calculated values for the similar dissociation of Me_3ZnLi in Me_2O.[40] It should be mentioned that Li^+ is known to adopt the tetrasolvated solid-state structure $[Li(THF)_4]^+$.[41] However, a dissociation process that straightforwardly generates a tetrasolvated Li^+ is inconceivable because the alkali metal of Et_3ZnLi can be coordinated by three THF molecules at most and not four (See Scheme SI.9), for steric congestion reasons. Therefore, $[Li(THF)_4]^+$ should be produced by subsequent exergonic solvation of $[Li(THF)_2]^+$ resulting from the dissociation of **C**, that is in a secondary process which cannot be honestly viewed as a part of the dissociation step (Schemes 10 and SI.9). **M** and **1a** generate the association complex **CP_{3a}** with a 3.2 kcal/mol energy loss (pathway 3a) while $[Li(THF)_4]^+$ acts as a spectator ion. Then, the migration of one of the Et groups to the σ-hole of iodine atom occurs with a 10.9 kcal/mol endergonicity (**TS_{3a}**). The migration of the aryl moiety to the Zn centre and decoordination of EtI from the same metal centre furnish **P_{2a}** which is 27.8 kcal/mol lower in Gibbs free energy than **TS_{3a}**. The Gibbs free activation energy, added to Gibbs free energy of dissociation associated with the formation **M** and **CP_{3a}** (sum = 31.7 kcal/mol), discredits this anionic pathway. Saturation of coordination sphere of the Zn centre with a THF molecule (pathway 3b) does not change the conclusion.

Conclusions

In summary, we have conducted a detailed computational study of the I/Zn exchange reaction of 4-iodobenzyl mesylate with lithium triethylzincate. To date, it represents the first in-depth investigation of such a reaction involving (1) an iodoaryl

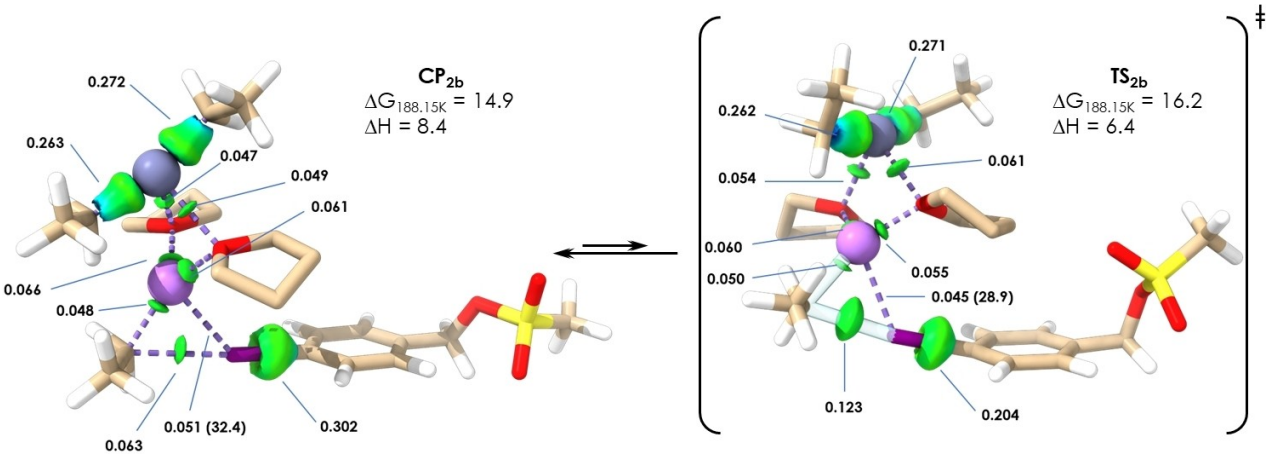

Scheme 9. 3D representation of the open form **CP_{2b}** and the related localised transition states **TS_{2b}** leading to **Int_{1a}** including related IBSI values (Energies values in kcal/mol, E(2) energies in parentheses. Zinc atom is represented as a blue sphere and lithium atom as a purple sphere, hydrogen atoms of THF molecules are omitted for better clarity).

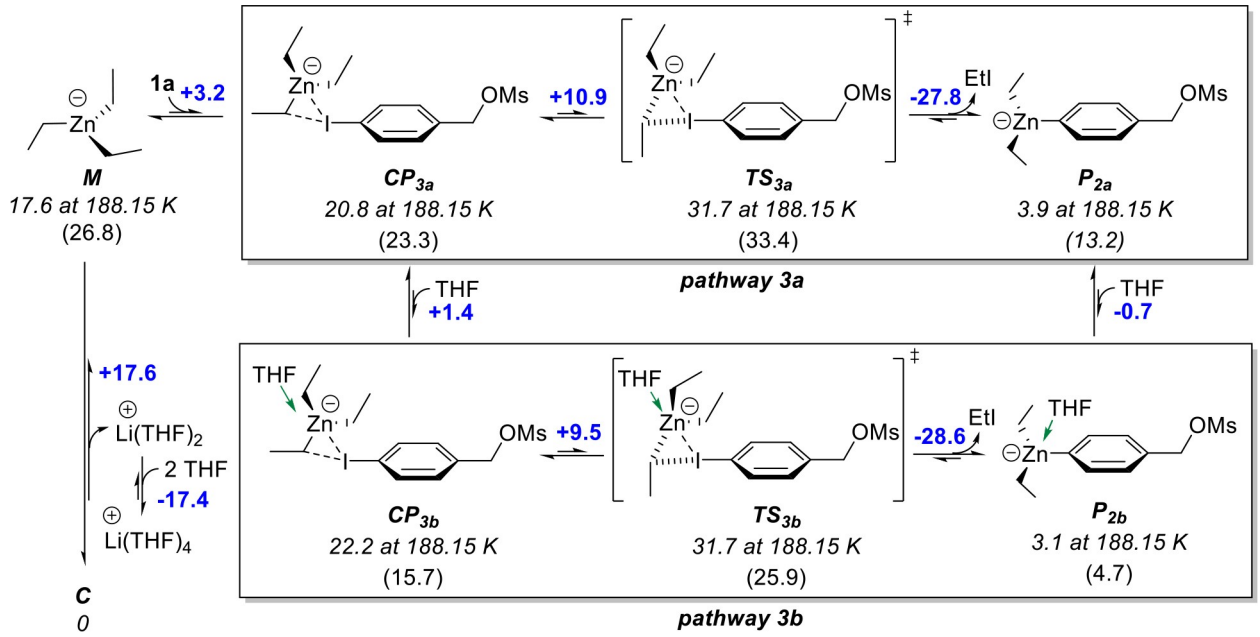

Scheme 10. Anionic pathway calculated at the IEFPCM/M06-2X-D3/cc-pVDZ (SDD for I) level of theory (Gibbs free energies at 188.15 K and enthalpies in parentheses are specified in kcal/mol. ΔG° are accessible in the SI).

as substrate, (2) THF as commonly used solvent in this kind of reaction (3) the presence of a potential *para*-directing group. A microsolvation approach[18] was adopted during the whole investigation. Such an approach likely surpasses those based only on implicit solvent models as it enabled us to highlight under-estimated, if not unknown, explicit solute-solvent interactions that can strongly influence the reactivity of Et_3ZnLi. First and foremost, we established that the previously experimentally defined composition for this reagent in a THF solution ($Et_3ZnLi \cdot 2THF$)[27] referred to the most thermodynamically stable specie **C** where two THF molecules are coordinated to Li (Scheme 2). Secondly, interconnected dynamic equilibria between **C** and other differently solvated complexes, such as **C**⇌**B**, **C**⇌**E**, **C**⇌**F**⇌**G**⇌**I** could easily operate. Thirdly, this approach, in combination with a thorough examination of IBSI, offers a new look on the behaviour of Et_3ZnLi when placed in a THF solution. For the first time, **C** could clearly be defined as a versatile species in which alkali metal was moving between its two L-type C_{Et} ligand in order to produce **F**. This resulted in considering **C** and **F** as limit forms of $Et_3ZnLi \cdot 2THF$ (Figure 1), the former displaying the highest statistical weight. This structural versatility was also illustrated by another limit form **G** that could not have been localised by only using implicit solvent models. **G** is a unique unreported organometallic species consisting of two complexes, namely Et_2Zn and EtLi, and two solvent molecules for stabilising the heterodinuclear species. As Zn interacts very weakly with Li, **G** can be viewed as a THF-solvated open zincate complex. Since IBSI analysis for **C** as well as reported data deduced from solid-state structural analysis for lithium trialkylzincates suggest that alkyl ligand is covalently attached to Zn centre[34] **G** should be characterised by a statistical weight drastically lower than that of **F** and **C**. Based on these identified equilibria, three mechanistic routes including 10 sub-pathways were examined, namely a standard pathway with preserved synergic character of Et_3ZnLi and with or without initial coordination of Li to OMs group (pathway 1), a THF-solvated open zincate complex-promoted pathway (pathway 2) and an anionic pathway (pathway 3). The thermodynamic profile of the most relevant pathways is displayed in Scheme 11. Anionic pathway 3 is totally precluded. The two other pathways involve a transition state including a hypervalent iodine-type structure stabilised by interaction between the electron lone pair of the iodine atom and the vacant orbital of lithium. Examination of selected suitable Kohn-Sham orbitals indicated the existence of a three-centre four-electron bond which is typical of such a structure. Amazingly, our microsolvation approach-based study led to the original conclusion that pathway 2 was by far the most energetically favourable in THF. Considering a thermodynamic profile with enthalpy values instead of Gibbs free energy values does not alter this conclusion (Scheme SI.10). This pathway preliminarily requires the formation of the THF-solvated open zincate complex **G** that should be viewed as a transient species. The solvent being integral to the structure of **G**, it is also integral to the mechanism associated with this pathway. Accordingly, it is not surprising that strong solvent effects could be observed experimentally, including when the molecular structure of the solvent is marginally different from THF (*e.g.* 2-MeTHF).[20] Pathway 1e displaying an initial coordination of the reagent to OMs through its Li atom is only insignificantly lower in energy than pathway 1a proceeding without such a chemical event. This suggests that (1) a benzylic bulky directing group positioned at the *para* position with respect to halogen has no major influence on the course of the reaction and (2) both

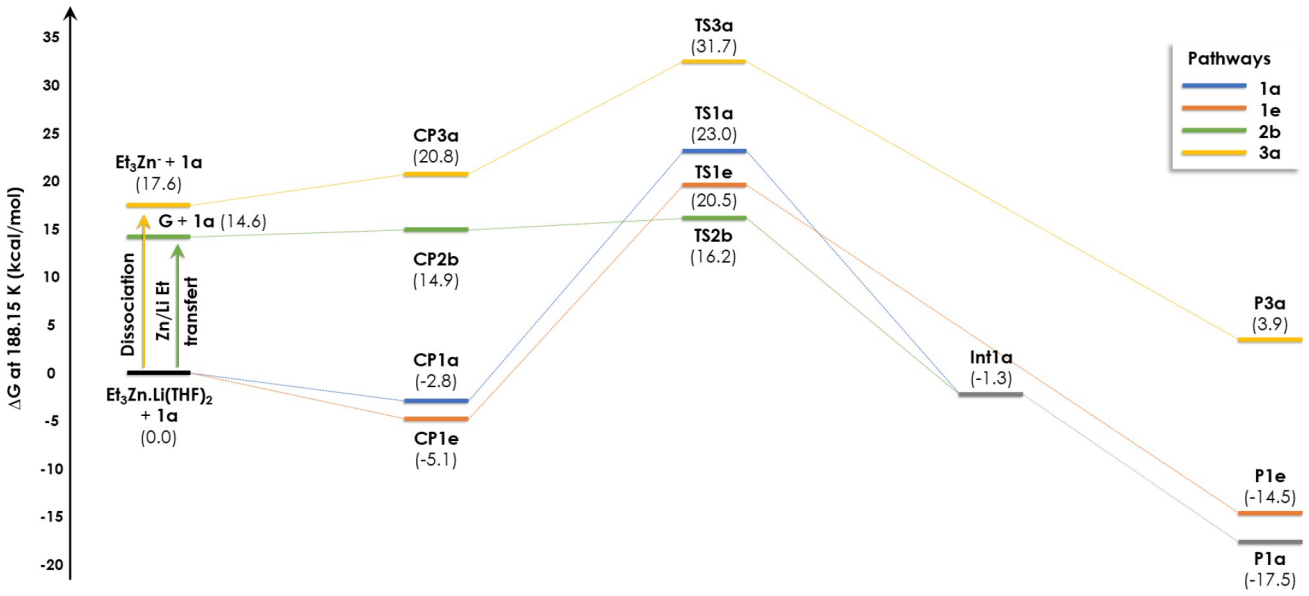

Scheme 11. Thermodynamic profile of the most relevant pathways calculated for the Zn/I exchange reaction at the IEFPCM/M06-2X-D3/cc-pVDZ (SDD for I) level of theory (Gibbs free energies at 188.15 K in kcal/mol).

pathways 1a and 1e have to be viewed as complementary. Finally, we demonstrated that the I/Zn exchange reaction proceeded through a two step-mechanism where the lithium zincate actually acted as a converter of iodoaryl into the corresponding aryllithium compound. First the iodoaryl substrate is converted into aryllithium intermediate which was localised for the first time. Then, this generated aryllithium and the remaining diethylzinc associated with the former by two THF molecules react together through transmetallation so as to furnish the I/Zn exchange reaction product. This 2-step process echoes the so-called trans-metal-trapping mechanism proposed for the deprotonation/ metalation of anisole and other arenes with LiTMP-Zn(TMP)$_2$ as reagent.[38]

Experimental Section

Computational details: All structures were fully optimized with the at the Density Functional Theory (DFT) level with the M06-2X functional[21] and the cc-pVDZ basis set[22] for all atoms except I where Effective Core Potential (ECP) card was used with the Stuttgart/Dresden (SDD) basis set.[42] The SDD effective core potential (ECP) has been recently proved to be the best method with iodide containing organic compounds especially with hypervalent iodines.[43] Moreover, it is worth mentioning that the choice of the M06-2X functional was made based on the extensive benchmark studies by Amin's group (for Zn)[44] and Pratt's group (for Li).[45] D3 version of Grimme's dispersion with the original D3 damping function[23] was added for all calculations. The nature of all extrema as minimum or transition state was characterized with analytical calculations of frequencies at 1 atm and at 298.15 and 188.15 K to mimic the experimental conditions. Transition states were connected to reactants and products with Intrinsic Reaction Coordinate (IRC) calculations. Transition states were located using synchronous Transit-Guided Quasi-Newton method (STQN)[46] and fully optimized using Berny algorithm. In addition to the solvent molecules bound to metals, implicit solvation was modelled by using the IEFPCM[24] solvation model (tetrahydrofuran, THF, with ε of 7.58). All calculations were performed with the Gaussian16 revision B.01 program packages. IGMPlot software[47] has been used to extract the weak interactions between the considered molecular fragments based on the Independent gradient model (IGM)[35b] of the wavefunction obtained from QM calculations. IGMPlot software was used to determine the intrinsic bond strength index (IBSI) of organic ligand - metal bonds. NBO 6.0 programme[48] was employed to quantify donor-acceptor interactions via the second order perturbation theory analysis. ChimeraX 1.6.1[49] and CYLview 1.0b[50] softwares were used to visualize calculated Contact Pairs (**CP**), Transitions States (**TS**), Aryl lithium INTermediates (**INT**) and products (**P**).

General information for analytical experiments: *n*-BuLi (1.6 M in hexanes) and EtLi (0.5 M in benzene) are commercially obtained from Acros and titrated under argon atmosphere by using a dry toluene solution of menthol and 2,2′-bipyridine as indicator. Anhydrous $ZnCl_2$ (>98% reagent grade) is commercially available and was used as received. All starting materials **1a–c** were prepared from 4-Iodobenzyl alcohol purchased from Aldrich and according standard procedures. **1a** was synthesised by mesylation of the corresponding benzyl alcohol using DMAP (0.1 equiv.)/Et_3N (2 equiv.)/MsCl at −10 °C in DCM for 1 h and subsequent quench with HCl-1M.[51] **1c** was prepared according the same procedure as that for **1a** but after the 1-hour period at −10 °C, the reaction mixture was stirred at rt overnight before quench with HCl-1M. **1b** was obtained by treatment of 4-Iodobenzyl alcohol with Me_3SiBr (1.5 equiv.) at rt in DCM for 12 h and subsequent quench with water.[52] Experimental data relating to **1a–c** were identical to those reported.[53] Reactions reported in Scheme 6 were carried out under an atmosphere of argon, with dry oxygen-free organic solvent and using standard Schlenk techniques. All solvents and liquid reagents were transferred using plastic single-use graduated syringes and stainless-steel needles. THF (HPLC grade, non-stabilized, BioLab) was dried using Solvent Purifier System (SPS Mbraun 800) (two columns of alumina) and kept under positive pressure of argon (99.9999% purity grade).

General procedure for 2a–c: An oven-dried 50 mL-three-neck flask, equipped with a Teflon coated magnetic stir bar, a greased gas

inlet adaptor with a glass plug, a rubber septum and a low-temperature thermometer with greased glass adaptor, was preliminarily charged with anhydrous $ZnCl_2$ (164 mg, 1.2 mmol, 2.0 equiv.). The flask was connected to the Schlenk line and the air was pumped out of the flask. $ZnCl_2$ was heated three times using a heat gun. Once the flask returned to room temperature, the resulting vacuum was replaced with argon. This "vac-refill" operation was performed three times. Dry THF (8 mL) was added and the resulting mixture was stirred at −10 °C for 10 min. A solution of *n*-butyllithium (1.6 M in hexanes, 2.13 ml, 3.4 mmol) was then added dropwise under inert atmosphere at that temperature. After a 20 min-stirring period at −10 °C, the reaction mixture was cooled down to −85 °C. A 2 mL dry THF solution of 4-iodobenzyl derivative **1** (0.6 mmol, 1.0 equiv.) was added dropwise and the reaction mixture was stirred at −85 °C for 30 min. Finally, the reaction mixture was hydrolyzed with an aqueous solution of 1 M HCl (1 mL) at that temperature. The layers were separated and the aqueous phase was extracted with EtOAc (3 times). The combined organic fractions were washed with brine, dried over MgSO4, filtered and concentrated under reduced pressure. Conversion of 1 into 2 was determined by GC/MS analysis of the crude mixture in EtOAc.

Supporting Information

The authors have cited additional references within the Supporting Information.[54,55,56,57,58]

Acknowledgements

The authors thank the French "Agence Nationale de Recherche" (ANR-19-CE07-0032) for financial support and grants to A.P. We gratefully acknowledge the MaSCA (Maison de la Simulation de Champagne-Ardenne, France) and the P3 M (Plateau de Modélisation Moléculaire Multi-échelles, Reims, France) for computational facilities. Dr. Francesca Ingrosso (Université de Lorraine, CNRS, LPCT, F-54000 Nancy, France) is warmly thanked for discussions and proofreading.

Conflict of Interests

The authors declare no conflict of interest.

Data Availability Statement

The data that support the findings of this study are available from the corresponding author upon reasonable request.

Keywords: zincate · halogen · metal exchange · DFT · microsolvation · heterobimetallic reagent

[1] For the synthetic importance of the Li/halogen exchange transformation, see: a) K. Inoue, K. Okano, *Asian J. Org. Chem.* **2020**, *9*, 1548–1561; For Zn/halogen exchange, see: b) M. Balkenhohl, P. Knochel, *Chem. Eur. J.* **2020**, *26*, 3688–3697; For other halogen/metal exchange transformations, see: c) D. Tilly, F. Chevallier, F. Mongin, P. C. Gros, *Chem. Rev.* **2014**, *114*, 1207–1257.

[2] R. G. Jones, H. Gilman, *Org. React.* **1951**, *6*, 339–366.

[3] For reviews, see: a) "The Halogen-Metal Interconversion and Related Processes (M = Li, Mg)": F. R. Leroux, A. Panossian in *Arene Chemistry: Reaction Mechanisms and Methods for Aromatic Compounds* (Ed: J. Mortier), Wiley, Hoboken, **2015**, p. 813–833; b) H. J. Reich, *Chem. Rev.* **2013**, *113*, 7130–7178; c) W. F. Bailey, J. J. Patricia, *J. Organomet. Chem.* **1988**, *352*, 1–46.

[4] G. Wittig, U. Schçllkopf, *Tetrahedron* **1958**, *3*, 91–93.

[5] a) G. A. Russell, D. W. Lamson, *J. Am. Chem. Soc.* **1969**, *91*, 3967–3968; b) H. Fischer, *J. Phys. Chem.* **1969**, *73*, 3834–3838.

[6] S. V. Sunthankar, H. Gilman, *J. Org. Chem.* **1951**, *16*, 8–16.

[7] G. Wittig, *Angew. Chem.* **1958**, *70*, 65–71.

[8] N. S. Zefirov, D. I. Makhon'kov, *Chem. Rev.* **1982**, *82*, 615–624.

[9] H. J. Reich, *J. Org. Chem.* **2012**, *77*, 5471–5491.

[10] a) H. J. Reich, W. L. Whipple, *Can. J. Chem.* **2005**, *83*, 1577–1587; b) M. Müller, H.-C. Stiasny, M. Brönstrup, A. Burton, R. W. Hoffmann, *J. Chem. Soc.-Perkin Trans.* **1999**, *2*, 731–736; c) H. J. Reich, D. P. Green, N. H. Phillips, *J. Am. Chem. Soc.* **1991**, *113*, 1414–1416; d) H. J. Reich, D. P. Green, N. H. Phillips, *J. Am. Chem. Soc.* **1989**, *111*, 3444–3445.

[11] a) K. Ando, *J. Org. Chem.* **2006**, *71*, 1837–1850; b) K. B. Wiberg, S. Sklenak, W. F. Bailey, *Organometallics* **2001**, *20*, 771–774; c) K. B. Wiberg, S. Sklenak, W. F. Bailey, *J. Org. Chem.* **2000**, *65*, 2014–2021; d) G. Boche, M. Schimeczek, J. Cilowski, P. Piskorz, *Eur. J. Org. Chem.* **1998**, *1998*, 1851–1860; e) B. Jedlicka, R. H. Crabtree, E. M. Siegbahn, *Organometallics* **1997**, *16*, 6021–6023.

[12] W. B. Farnham, J. C. Calabrese, *J. Am. Chem. Soc.* **1986**, *108*, 2449–2451.

[13] a) S. D. Robertson, M. Uzelac, R. E. Mulvey, *Chem. Rev.* **2019**, *119*, 8332–8405; b) A. Harrison-Marchand, F. Mongin, *Chem. Rev.* **2013**, *113*, 7470–7562; c) R. P. Davies, *Coord. Chem. Rev.* **2011**, *255*, 1226–1251.

[14] T. D. Bluemke, W. Clegg, P. García-Alvarez, A. R. Kennedy, K. Koszinowski, M. D. McCall, L. Russo, E. Hevia, *Chem. Sci.* **2014**, *5*, 3552–3562.

[15] The 1:3 mixture of $ZnCl_2$·TMEDA and LiTMP in THF mainly leads to LiTMP and $(TMP)_2Zn$, see: a) A. Seggio, M.-I. Lannou, F. Chevallier, D. Nobuto, M. Uchiyama, S. Golhen, T. Roisnel, F. Mongin, *Chem. Eur. J.* **2007**, *13*, 9982–9989; b) J.-M. L'Helgoual'ch, A. Seggio, F. Chevallier, M. Yonehara, E. Jeanneau, M. Uchiyama, F. Mongin, *J. Org. Chem.* **2008**, *73*, 177–183.

[16] a) M. Uzelac, A. R. Kennedy, E. Hevia, R. E. Mulvey, *Angew. Chem. Int. Ed.* **2016**, *55*, 13147–13150; *Angew. Chem.* **2016**, *128*, 13341–13344; b) D. R. Armstrong, E. Crosbie, E. Hevia, R. E. Mulvey, D. L. Ramsay, S. D. Robertson, *Chem. Sci.* **2014**, *5*, 3031–3045; c) D. R. Armstrong, A. R. Kennedy, R. E. Mulvey, J. A. Parkinson, S. D. Robertson, *Chem. Sci.* **2012**, *3*, 2700–2707; d) P. García-Álvarez, R. E. Mulvey, J. A. Parkinson, *Angew. Chem. Int. Ed.* **2011**, *50*, 9668–9671; *Angew. Chem.* **2011**, *123*, 9842–9845.

[17] a) H. J. Reich, N. H. Phillips, I. L. Reich, *J. Am. Chem. Soc.* **1985**, *107*, 4101–4103; b) H. R. Rogers, J. Houk, *J. Am. Chem. Soc.* **1982**, *104*, 522–525; c) H. J. S. Winkler, H. Winkler, *J. Am. Chem. Soc.* **1966**, *88*, 969–974; d) H. J. S. Winkler, H. Winkler, *J. Am. Chem. Soc.* **1966**, *88*, 964–968; e) D. E. Applequist, D. F. O Brien, *J. Am. Chem. Soc.* **1963**, *85*, 743–748.

[18] J. Rio, L. Perrin, P.-A. Payard, *Eur. J. Org. Chem.* **2022**, *2022*, e202200906.

[19] a) S. Nakamura, C.-Y. Liu, A. Muranaka, M. Uchiyama, *Chem. Eur. J.* **2009**, *15*, 5686–5694; b) A. Krasovskiy, B. F. Straub, P. Knochel, *Angew. Chem. Int. Ed.* **2006**, *45*, 159–162; *Angew. Chem.* **2006**, *118*, 165–169.

[20] a) A. Pierret, C. Denhez, P. C. Gros, A. Vasseur, *Adv. Synth. Catal.* **2022**, *364*, 3805–3816; b) T. Harada, T. Kaneko, T. Fujiwara, A. Oku, *J. Org. Chem.* **1997**, *62*, 8966–8967.

[21] Y. Zhao, D. G. Truhlar, *Theor. Chem. Acc.* **2008**, *120*, 215–241.

[22] a) T. H. Dunning Jr, *J. Chem. Phys.* **1989**, *90*, 1007–1023; b) E. R. Davidson, *Chem. Phys. Lett.* **1996**, *260*, 514–518.

[23] S. Grimme, J. Antony, S. Ehrlich, J. Krieg, *J. Chem. Phys.* **2010**, *132*, 154104.

[24] V. Barone, M. Cossi, J. Tomasi, *J. Chem. Phys.* **1997**, *107*, 3210–3221.

[25] a) S. R. Boss, M. P. Coles, R. Haigh, P. B. Hitchcock, R. Snaith, A. E. H. Wheatley, *Angew. Chem. Int. Ed.* **2003**, *42*, 5593–5596; *Angew. Chem.* **2003**, *115*, 5751–5754; b) "hpp" means hexahydropyrimidopyrimidine.

[26] a) E. Weiss, *Angew. Chem. Int. Ed. Engl.* **1993**, *32*, 1501–1523; *Angew. Chem.* **1993**, *105*, 1565–1587; b) A. P. Purdy, C. F. George, *Organometallics* **1992**, *11*, 1955–1959.

[27] S. Toppet, G. Slinckx, G. Smets, *J. Organomet. Chem.* **1967**, *9*, 205–213.

[28] K. Koszinowski, P. Böhrer, *Organometallics* **2009**, *28*, 100–110.

[29] For Li, see: a) E. Rijnberg, J. T. B. H. Jastrzebski, J. Boersma, H. Kooijman, N. Veldman, A. L. Spek, G. van Koten, *Organometallics* **1997**, *16*, 2239–2245; For other metal cation, see: b) M. Westerhausen, C. Gückel, H. Piotrowski, M. Vogt, *Z. Anorg. Allg. Chem.* **2002**, *628*, 735–740; c) M.

Westerhausen, C. Gückel, T. Habereder, M. Vogt, M. Warchhold, H. Nöth, *Organometallics* **2001**, *20*, 893–899; d) M. Krieger, G. Geiseler, K. Harms, J. Merle, W. Massa, K. Dehnicke, *Z. Anorg. Allg. Chem.* **1998**, *624*, 1387–1388; e) K. H. Thiele, H. Görls, W. Seidel, *Z. Anorg. Allg. Chem.* **1998**, *624*, 555–556.
[30] M. A. Putzner, B. Neumüller, K. Dehnicke, *Z. Anorg. Allg. Chem.* **1997**, *623*, 539–544.
[31] M. Uchiyama, S. Nakamura, T. Furuyama, E. Nakamura, K. Morokuma, *J. Am. Chem. Soc.* **2007**, *129*, 13360–13361.
[32] M. Uchiyama, S. Nakamura, T. Ohwada, M. Nakamura, E. Nakamura, *J. Am. Chem. Soc.* **2004**, *126*, 10897–10903.
[33] J. Klein, H. Khartabil, J.-C. Boisson, J. Contreras-García, J.-P. Piquemal, E. Hénon, *J. Phys. Chem. A* **2020**, *124*, 1850–1860.
[34] a) M. Dell'Aera, F. Maria Perna, P. Vitale, A. Altomare, A. Palmieri, L. C. H. Maddock, L. J. Bole, A. R. Kennedy, E. Hevia, V. Capriati, *Chem. Eur. J.* **2020**, *26*, 8742–8748; b) D. R. Armstrong, J. García-Álvarez, D. V. Graham, G. W. Honeyman, E. Hevia, A. R. Kennedy, R. E. Mulvey, *Chem. Eur. J.* **2009**, *15*, 3800–3807.
[35] a) C. Lefebvre, H. Khartabil, J.-C. Boisson, J. Contreras-García, J.-P. Piquemal, E. Hénon, *ChemPhysChem* **2018**, *19*, 724–735; b) C. Lefebvre, G. Rubez, H. Khartabil, J.-C. Boisson, J. Contreras-García, E. Hénon, *Phys. Chem. Chem. Phys.* **2017**, *19*, 17928–17936.
[36] For reviews on the concept of σ-hole interactions, see: a) W. Zierkiewicz, M. Michalczyk, S. Scheiner, *Molecules* **2021**, *26*, 1740; b) P. Scilabra, G. Terraneo, G. Resnati, *Acc. Chem. Res.* **2019**, *52*, 1313–1324; c) P. Politzer, J. S. Murray, *Crystals* **2017**, *7*, 212; d) P. Politzer, J. S. Murray, T. Clark, *Phys. Chem. Chem. Phys.* **2013**, *15*, 11178–11189; For applications in catalysis, see: e) M. Breugst, J. J. Koenig, *Eur. J. Org. Chem.* **2020**, *2020*, 5473–5487.
[37] S. Yannacone, V. Oliveira, N. Verma, E. Kraka, *Inorganics* **2019**, *7*, 47.
[38] Although not reported for the lithium zincate promoted I/Zn exchange, this process reminds the *trans*-metal-trapping mechanism proposed for the deprotonation/metalation of arenes unsing LiTMP–$Zn(TMP)_2$ as reagent, see: a) G. Akimoto, M. Otsuka, R. Takita, M. Uchiyama, M. Hedidi, G. Bentabed-Ababsa, F. Lassagne, W. Erb, F. Mongin, *J. Org. Chem.* **2018**, *83*, 13498–13506; b) N. Brikci-Nigassa, G. Bentabed-Ababsa, W. Erb, F. Mongin, *Synthesis* **2018**, *50*, 3615–3633.
[39] K. Koszinowski, P. Böhrer, *Organometallics* **2009**, *28*, 771–779.
[40] This Gibbs free energy found for such a dissociation corresponds to a 29.2 kcal/mol electronic energy. The latter should be compared with the 127.4 kcal/mol value reported in Ref [19a] for the dissociation of $Me_3ZnLi{\cdot}OMe_2$ into $[Me_3Zn]^-$ and $[Li(OMe)]^+$.
[41] R. Fischer, H. Schmidt, F. M. Younis, H. Görls, R. Suxdorf, M. Westerhausen, *Z. Anorg. Allg. Chem.* **2020**, *646*, 207–214.
[42] X. Y. Cao, M. Dolg, *J. Chem. Phys.* **2001**, *115*, 7348–755.
[43] K. Matsumoto, M. Nakajima, T. Nemoto, *J. Phys. Org. Chem.* **2019**, *32*, e3961.
[44] E. A. Amin, D. G. Truhlar, *J. Chem. Theory Comput.* **2008**, *4*, 75–85.
[45] B. R. Ramachandran, L. M. Pratt, Computational perspectives on organolithium carbenoids in Practical Aspects of Computational Chemistry II **2012**, Springer, Dordrecht pp. 471–510.
[46] a) C. Peng, H. B. Schlegel, *Isr. J. Chem.* **1993**, *33*, 449–454; b) C. Peng, P. Y. Ayala, H. B. Schlegel, M. J. Frisch, *J. Comb. Chem.* **1996**, *17*, 49–56.
[47] C. Lefebvre, J. Klein, H. Khartabil, J.-C. Boisson, E. Hénon, *J. Comb. Chem.* **2023**, *44*, 1750–1766.
[48] E. D. Glendening, C. R. Landis, F. Weinhold, *J. Comput. Chem.* **2013**, *14*, 1429–1437.
[49] E. F. Pettersen, T. D. Goddard, C. C Huang, E. C. Meng, G. S. Couch, T. I. Croll, J. H. Morris, T. E. Ferrin, *Protein Sci.* **2021**, *30*, 70–82.
[50] C. Y. Legault, Université de Sherbrooke, 2009 (http://www.cylview.org).
[51] C. Chardin, J. Rouden, S. Livi, J. Baudoux, *Green Chem.* **2017**, *19*, 5054–5059.
[52] A. N. Pinchuk, M. A. Rampy, M. A. Longino, R. W. Scott Skinner, M. D. Gross, J. P. Weichert, R. E. Counsell, *J. Med. Chem.* **2006**, *49*, 2155–2165.
[53] For the synthesis of **1 a**, see: a) L. B. de O. Freitas, T. F. Borgati, R. P. de Freitas, A. L. T. G. Ruiz, G. M. Marchetti, J. E. de Carvalho, E. F. F. da Cunha, T. C. Ramalho, R. B. Alves, *Eur. J. Med. Chem.* **2014**, *84*, 595–604; For **1 b**, see: b) ref [41]; For **1 c**, see: c) H.-W. Kim, Y.-S. Lee, D. Shetty, H.-J. Lee, D.-S. Lee, J.-K. Chung, M.-C. Lee, K.-H. Chung, J.-M. B. Jeong, *Bull. Korean Chem. Soc.* **2010**, *31*, 3434–3436.
[54] C. J. Cramer, D. G. Truhlar, *Phys. Chem. Chem. Phys.* **2009**, *11*, 10757–10816.
[55] C. Demangeat, T. Saied, R. Ramozzi, F. Ingrosso, M. Ruiz-Lopez, A. Panossian, F. R. Leroux, Y. Fort, C. Comoy, *Eur. J. Org. Chem.* **2019**, *2019*, 547–556.
[56] S. Grimme, A. Hansen, J. G. Brandenburg, C. Bannwarth, *Chem. Rev.* **2016**, *116*, 5105–5154.
[57] T. Lu, *J. Comput. Chem.* **2012**, *33*, 580–592.
[58] J. Zhang, T. Lu, *Phys. Chem. Chem. Phys.* **2021**, *23*, 20323–20328.